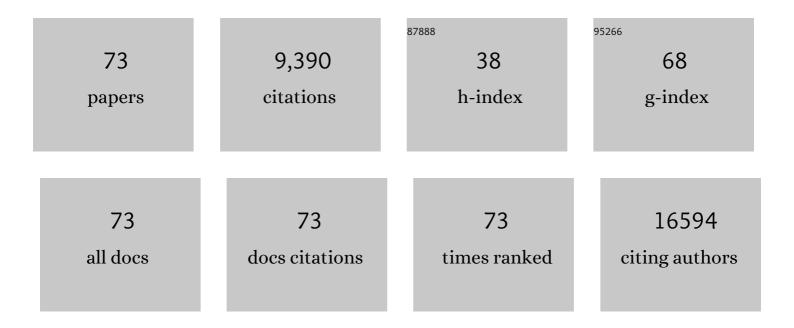
## Ai Leen Koh

List of Publications by Year in descending order

Source: https://exaly.com/author-pdf/8134274/publications.pdf Version: 2024-02-01



ALLEEN KOH

#	Article	IF	CITATIONS
1	Activating and optimizing MoS2 basal planes for hydrogen evolution through the formation of strained sulphur vacancies. Nature Materials, 2016, 15, 48-53.	27.5	2,021
2	Atomic structure of sensitive battery materials and interfaces revealed by cryo–electron microscopy. Science, 2017, 358, 506-510.	12.6	1,039
3	Quantum plasmon resonances of individual metallic nanoparticles. Nature, 2012, 483, 421-427.	27.8	991
4	Observation of Quantum Tunneling between Two Plasmonic Nanoparticles. Nano Letters, 2013, 13, 564-569.	9.1	472
5	Particle Size, Surface Coating, and PEGylation Influence the Biodistribution of Quantum Dots in Living Mice. Small, 2009, 5, 126-134.	10.0	418
6	Electron Energy-Loss Spectroscopy (EELS) of Surface Plasmons in Single Silver Nanoparticles and Dimers: Influence of Beam Damage and Mapping of Dark Modes. ACS Nano, 2009, 3, 3015-3022.	14.6	322
7	Electron microscopy of gold nanoparticles at atomic resolution. Science, 2014, 345, 909-912.	12.6	269
8	In situ detection of hydrogen-induced phase transitions in individual palladium nanocrystals. Nature Materials, 2014, 13, 1143-1148.	27.5	261
9	High-Resolution Mapping of Electron-Beam-Excited Plasmon Modes in Lithographically Defined Gold Nanostructures. Nano Letters, 2011, 11, 1323-1330.	9.1	253
10	Kinetic Study of Hydrogen Evolution Reaction over Strained MoS <sub>2</sub> with Sulfur Vacancies Using Scanning Electrochemical Microscopy. Journal of the American Chemical Society, 2016, 138, 5123-5129.	13.7	244
11	Real-Time Intravital Imaging of RGDâ^'Quantum Dot Binding to Luminal Endothelium in Mouse Tumor Neovasculature. Nano Letters, 2008, 8, 2599-2606.	9.1	207
12	Pro-efferocytic nanoparticles are specifically taken up by lesional macrophages and prevent atherosclerosis. Nature Nanotechnology, 2020, 15, 154-161.	31.5	173
13	Construction and Validation of Nano Gold Tripods for Molecular Imaging of Living Subjects. Journal of the American Chemical Society, 2014, 136, 3560-3571.	13.7	170
14	Multiplex Detection of Protease Activity with Quantum Dot Nanosensors Prepared by Intein-Mediated Specific Bioconjugation. Analytical Chemistry, 2008, 80, 8649-8655.	6.5	163
15	Controlling sulphur precursor addition for large single crystal domains of WS <sub>2</sub> . Nanoscale, 2014, 6, 12096-12103.	5.6	149
16	Surface Monocrystallization of Copper Foil for Fast Growth of Large Singleâ€Crystal Graphene under Free Molecular Flow. Advanced Materials, 2016, 28, 8968-8974.	21.0	128
17	A Metafluid Exhibiting Strong Optical Magnetism. Nano Letters, 2013, 13, 4137-4141.	9.1	121
18	X-ray-Induced Shortwave Infrared Biomedical Imaging Using Rare-Earth Nanoprobes. Nano Letters, 2015, 15, 96-102.	9.1	120

Ai Leen Koh

#	Article	IF	CITATIONS
19	Rapid Flame Synthesis of Atomically Thin MoO <sub>3</sub> down to Monolayer Thickness for Effective Hole Doping of WSe <sub>2</sub> . Nano Letters, 2017, 17, 3854-3861.	9.1	120
20	Chemical and Phase Evolution of Amorphous Molybdenum Sulfide Catalysts for Electrochemical Hydrogen Production. ACS Nano, 2016, 10, 624-632.	14.6	109
21	Synthesis and characterization of PVP-coated large core iron oxide nanoparticles as an MRI contrast agent. Nanotechnology, 2008, 19, 165101.	2.6	108
22	Nature and Distribution of Stable Subsurface Oxygen in Copper Electrodes During Electrochemical CO <sub>2</sub> Reduction. Journal of Physical Chemistry C, 2017, 121, 25003-25009.	3.1	98
23	Surface Engineering of Copper Foils for Growing Centimeter-Sized Single-Crystalline Graphene. ACS Nano, 2016, 10, 2922-2929.	14.6	89
24	Revealing Nanoscale Passivation and Corrosion Mechanisms of Reactive Battery Materials in Gas Environments. Nano Letters, 2017, 17, 5171-5178.	9.1	88
25	Clean Transfer of Large Graphene Single Crystals for Highâ€Intactness Suspended Membranes and Liquid Cells. Advanced Materials, 2017, 29, 1700639.	21.0	80
26	Reconstructing solute-induced phase transformations within individual nanocrystals. Nature Materials, 2016, 15, 768-774.	27.5	72
27	Rapid Growth of Large Singleâ€Crystalline Graphene via Second Passivation and Multistage Carbon Supply. Advanced Materials, 2016, 28, 4671-4677.	21.0	69
28	High-performance oxygen reduction and evolution carbon catalysis: From mechanistic studies to device integration. Nano Research, 2017, 10, 1163-1177.	10.4	66
29	Improved QD-BRET conjugates for detection and imaging. Biochemical and Biophysical Research Communications, 2008, 372, 388-394.	2.1	61
30	van Hove Singularity Enhanced Photochemical Reactivity of Twisted Bilayer Graphene. Nano Letters, 2015, 15, 5585-5589.	9.1	59
31	Observations of Carbon Nanotube Oxidation in an Aberration-Corrected Environmental Transmission Electron Microscope. ACS Nano, 2013, 7, 2566-2572.	14.6	56
32	Cys-diabody Quantum Dot Conjugates (ImmunoQdots) for Cancer Marker Detection. Bioconjugate Chemistry, 2009, 20, 1474-1481.	3.6	52
33	High-Density 2D Homo- and Hetero- Plasmonic Dimers with Universal Sub-10-nm Gaps. ACS Nano, 2015, 9, 9331-9339.	14.6	51
34	Evolution of Plasmonic Metamolecule Modes in the Quantum Tunneling Regime. ACS Nano, 2016, 10, 1346-1354.	14.6	51
35	Distinguishing Oxygen Vacancy Electromigration and Conductive Filament Formation in TiO <sub>2</sub> Resistance Switching Using Liquid Electrolyte Contacts. Nano Letters, 2017, 17, 4390-4399.	9.1	50
36	Electron microscopy localization and characterization of functionalized composite organic-inorganic SERS nanoparticles on leukemia cells. Ultramicroscopy, 2008, 109, 111-121.	1.9	48

AI LEEN KOH

#	Article	IF	CITATIONS
37	Structure Determination of a Water-Soluble 144-Gold Atom Particle at Atomic Resolution by Aberration-Corrected Electron Microscopy. ACS Nano, 2017, 11, 11866-11871.	14.6	47
38	3D Reconstruction of VZV Infected Cell Nuclei and PML Nuclear Cages by Serial Section Array Scanning Electron Microscopy and Electron Tomography. PLoS Pathogens, 2012, 8, e1002740.	4.7	46
39	A Novel Method for Detection of Phosphorylation in Single Cells by Surface Enhanced Raman Scattering (SERS) using Composite Organic-Inorganic Nanoparticles (COINs). PLoS ONE, 2009, 4, e5206.	2.5	39
40	Tuning Chemical Potential Difference across Alternately Doped Graphene p–n Junctions for High-Efficiency Photodetection. Nano Letters, 2016, 16, 4094-4101.	9.1	34
41	Oxidation of Carbon Nanotubes in an Ionizing Environment. Nano Letters, 2016, 16, 856-863.	9.1	34
42	Visualizing Facet-Dependent Hydrogenation Dynamics in Individual Palladium Nanoparticles. Nano Letters, 2018, 18, 5357-5363.	9.1	31
43	Torsional Deformations in Subnanometer MoS Interconnecting Wires. Nano Letters, 2016, 16, 1210-1217.	9.1	30
44	Understanding the Active Sites of CO Hydrogenation on Pt–Co Catalysts Prepared Using Atomic Layer Deposition. Journal of Physical Chemistry C, 2018, 122, 2184-2194.	3.1	29
45	Formation and properties of magnetic chains for 100nm nanoparticles used in separations of molecules and cells. Journal of Magnetism and Magnetic Materials, 2009, 321, 1452-1458.	2.3	24
46	Efficient Radioisotope Energy Transfer by Gold Nanoclusters for Molecular Imaging. Small, 2015, 11, 4002-4008.	10.0	23
47	Intrinsic Chirality Origination in Carbon Nanotubes. ACS Nano, 2017, 11, 9941-9949.	14.6	23
48	Fabrication of planar, layered nanoparticles using tri-layer resist templates. Nanotechnology, 2011, 22, 185302.	2.6	22
49	Aberration-Corrected TEM Imaging of Oxygen Occupancy in YSZ. Journal of Physical Chemistry Letters, 2013, 4, 1156-1160.	4.6	22
50	The dissipation of field emitting carbon nanotubes in an oxygen environment as revealed by in situ transmission electron microscopy. Nanoscale, 2016, 8, 16405-16415.	5.6	19
51	Synthesis and characterization of graphite-encapsulated iron nanoparticles from ball milling-assisted low-pressure chemical vapor deposition. Carbon, 2017, 124, 170-179.	10.3	16
52	Rotating Anisotropic Crystalline Silicon Nanoclusters in Graphene. ACS Nano, 2015, 9, 9497-9506.	14.6	15
53	Assessing and ameliorating the influence of the electron beam on carbon nanotube oxidation in environmental transmission electron microscopy. Ultramicroscopy, 2017, 176, 132-138.	1.9	14
54	Spatial Variation of Available Electronic Excitations within Individual Quantum Dots. Nano Letters, 2013, 13, 716-721.	9.1	13

Ai Leen Koh

#	Article	IF	CITATIONS
55	Deciphering Surface Enhanced Raman Scattering Activity of Gold Nanoworms through Optical Correlations. Journal of Physical Chemistry C, 2011, 115, 20515-20522.	3.1	11
56	Rare-Earth-Doped Nanoparticles for Short-Wave Infrared Fluorescence Bioimaging and Molecular Targeting of α <sub>V</sub> β <sub>3</sub> -Expressing Tumors. Molecular Imaging, 2018, 17, 153601211879913.	1.4	10
57	The Stanford Nanocharacterization Laboratory (SNL) and Recent Applications of an Aberrationâ€Corrected Environmental Transmission Electron Microscope. Advanced Engineering Materials, 2014, 16, 476-481.	3.5	8
58	TEM analyses of synthetic anti-ferromagnetic (SAF) nanoparticles fabricated using different release layers. Ultramicroscopy, 2008, 108, 1490-1494.	1.9	7
59	Parallel preparation of plan-view transmission electron microscopy specimens by vapor-phase etching with integrated etch stops. Ultramicroscopy, 2016, 166, 39-47.	1.9	5
60	Preliminary Investigations of Chemical & Morphological Inhomogeneities in Laft6 Sro.4CoO3-δ Single-Crystalline Perovskite Thin Films by ACTEM and STEM-EELS. Microscopy and Microanalysis, 2015, 21, 1055-1056.	0.4	4
61	Atomic Resolution Observation of the Oxidation of Niobium Oxide Nanowires: Implications for Renewable Energy Applications. ACS Applied Nano Materials, 2020, 3, 9285-9292.	5.0	4
62	TEM Observations of Bio-Conjugated Streptavidin-Gold Nanoparticles. Materials Research Society Symposia Proceedings, 2007, 1019, 1.	0.1	3
63	Aberration-Corrected Transmission Electron Microscopy of the Intergranular Phase in Magnetic Recording Media. Nano Letters, 2012, 12, 2595-2598.	9.1	3
64	Antiphase Ordered Domains and Optical Diffraction for Copper-Gold and Samarium-doped Ceria: Reflections on Gareth Thomas. Microscopy and Microanalysis, 2016, 22, 1238-1239.	0.4	2
65	Evaluating Adhesion Layers for Plasmonic Nanostructures with Monochromated STEM-EELS and Surface Enhanced Raman Spectroscopy. Microscopy and Microanalysis, 2015, 21, 2055-2056.	0.4	1
66	In Situ Field Emission of Carbon Nanotubes in Oxygen Using Environmental TEM and the Influence of the Imaging Electron Beam. Microscopy and Microanalysis, 2017, 23, 910-911.	0.4	1
67	Contributions to High Resolution and In Situ Electron Microscopy. Microscopy and Microanalysis, 2018, 24, 10-11.	0.4	1
68	High Resolution In Situ and Transmission Environmental Electron Microscopy of Material Reactions. Microscopy and Microanalysis, 2019, 25, 3-4.	0.4	1
69	Scanning Electron Microscopy and Surface Enhanced Raman Spectroscopy Correlation Studies of Functionalized Composite Organic-Inorganic SERS Nanoparticles on Cancer Cells. Materials Research Society Symposia Proceedings, 2011, 1316, 1.	0.1	0
70	Oxidation Studies of Carbon Nanotubes for Applications as X-Ray Field Emitters Using an Aberration-Corrected, Environmental TEM. Microscopy and Microanalysis, 2013, 19, 466-467.	0.4	0
71	Imaging Perpendicular Magnetic Domains in Plan-view Using Lorentz Transmission Electron Microscopy. Microscopy and Microanalysis, 2014, 20, 286-287.	0.4	0
72	Unveiling the Atomistic Processes of the Accelerated Decomposition of 8.5 mol% Y2O3-stabilized ZrO2 by Environmental TEM. Microscopy and Microanalysis, 2017, 23, 2034-2035.	0.4	0

#	Article	IF	CITATIONS
73	Using Liquid Electrolytes in Dielectric Reliability Studies. , 2018, , .		Ο